Crack Growth Behavior of Irradiated Type 316 SS in Low Dissolved Oxygen Environment

Y. Chen[1], B. Alexandreanu[1], Y. Yang[2], W. J. Shack[1], K. Natesan[1],
E. E. Gruber[1], and A. S. Rao[3]

[1] Nuclear Engineering Division, Argonne National Laboratory;
9700 South Cass Ave., Argonne, IL 60439, USA
[2] Nuclear and Radiological Engineering Department, the University of Florida;
202 Nuclear Science Bldg., Gainesville, FL 32611, USA
[3] US Nuclear Regulatory Commission; Washington, DC 20555, USA

Keywords: IASCC, Stainless steels, BWR, HWC, Crack growth rate

Abstract

Cracking susceptibility of austenitic stainless steels is known to be affected by dissolved oxygen (DO) or corrosion potential. In low-DO environments, crack growth rate (CGR) is significantly lower than that in high-DO environment. A strong dependence of CGR on corrosion potential has also been seen in irradiated SSs. While it has been shown that reducing the potential can reduce the CGRs of irradiated SSs, some high-dose specimens have shown elevated CGRs even in low potential environments. Thus, it is not clear how irradiation affects the dependence of CGR on corrosion potential. In the present study, a disk-shaped compact tension specimen of Type 316 SS was tested in low-DO environment. The specimen was irradiated in the BOR-60 reactor to 5 dpa at 320°C. Post-irradiation CGR tests were performed in a low-DO environment. The effect of unloading on crack growth behavior in low-DO environment is discussed.

1. Introduction

Elevated cracking susceptibility is a key issue for austenitic stainless steels (SSs) in aging light water reactors (LWR). Exposed to both high temperature coolant and intensive neutron irradiation, stainless steel internal components can be susceptible to irradiation-assisted stress corrosion cracking (IASCC). Service failures of fuel cladding, internal structure, and fasteners have been seen in both boiling water reactors (BWR) and pressurized water reactors (PWRs) [1-4]. It has been shown that neutron irradiation plays a crucial role in this form of degradation. As neutron dose increases, non-sensitized SSs become increasingly vulnerable to stress corrosion cracking (SCC). For a given environment, a threshold-type behavior with increasing dose can be seen for IASCC [5-7]. There is no doubt that irradiation-induced microstructural and microchemical changes are the root cause of the elevated cracking susceptibility in SSs [8,9].

As a special form of stress corrosion cracking, IASCC is considered to have a similar dependence on environmental variables [10]. It has been shown in nonirradiated materials that SCC susceptibility depends strongly on the corrosion potential, and crack growth rate (CGR) in a low dissolved oxygen (DO) environment is significantly lower than that in a high-DO environment [10]. The low corrosion potential of BWR hydrogen water chemistry (HWC) or PWR primary water chemistry is considered beneficial and has been demonstrated to be an effective way to mitigate SCC [11,12]. For irradiated SSs, a similar correlation between CGR and corrosion potential has also been seen in many cases [13-15]. However, a systematic

analysis on the effect of low potential in irradiated materials is lacking. At present, CGR data for irradiated SSs in low-DO environments is limit. While in most cases, a beneficial effect of low-DO environments is observed, it has also been reported that CGR fails to respond to a decrease in potential in some high-dose specimens [13,16-18]. These observations seem to suggest that the mitigation of HWC may be only effective within a certain dose range. Even in cases where mitigation does occur, the effect of irradiation on the dependence of CGR on corrosion potential is also not well understood. A better understanding of the interaction between environmental and irradiation variables is needed to characterize crack growth behavior of irradiated SSs in low-DO environments.

In this study, a crack growth rate test was performed on an irradiated disk-shaped compact tension (DCT) specimen in a low-DO environment. Crack growth rates were measured under cyclic and constant-load condition to evaluate cracking susceptibility. Along with previous CGR results in low-DO environments, the effect of corrosion potential on crack growth behavior is discussed.

2. Experimental

2.1 Specimen and Irradiation

The CGR test was performed on a DCT specimen irradiated to 4.8 displacements per atom (dpa) at 320°C in BOR60 reactor through Cooperative IASCC Research (CIR) program [19]. The material (Heat BR) is a cold-worked (CW) Type 316 SS used for baffle bolts, and its chemical composition is given in Table 1. The BOR60 reactor is a sodium-cooled fast breeder reactor located at the Research Institute of Atomic Reactors (RIAR), Dimitrovgrad, Russia. The irradiation was carried out in sodium coolant between 315 and 325°C. After irradiation, the sodium was removed with a solution of ethanol-water mixture. The final damage dose was calculated by RIAR [19]. Figure 1 shows a schematic of the specimen with nominal dimensions. After irradiation, two side grooves of 5% of the thickness were added along the direction of crack advance.

Table 1. Chemical composition (wt.%) of CIR Heat BR.

Material	Heat	C	Mn	Si	P	S	Cr	Ni	Mo	N	Nb	Ti	O	Co	Cu
CW 316	BR	0.056	1.13	0.73	0.022	0.022	16.84	10.54	2.25	0.021	0.008	0.01	0.009	0.12	0.25

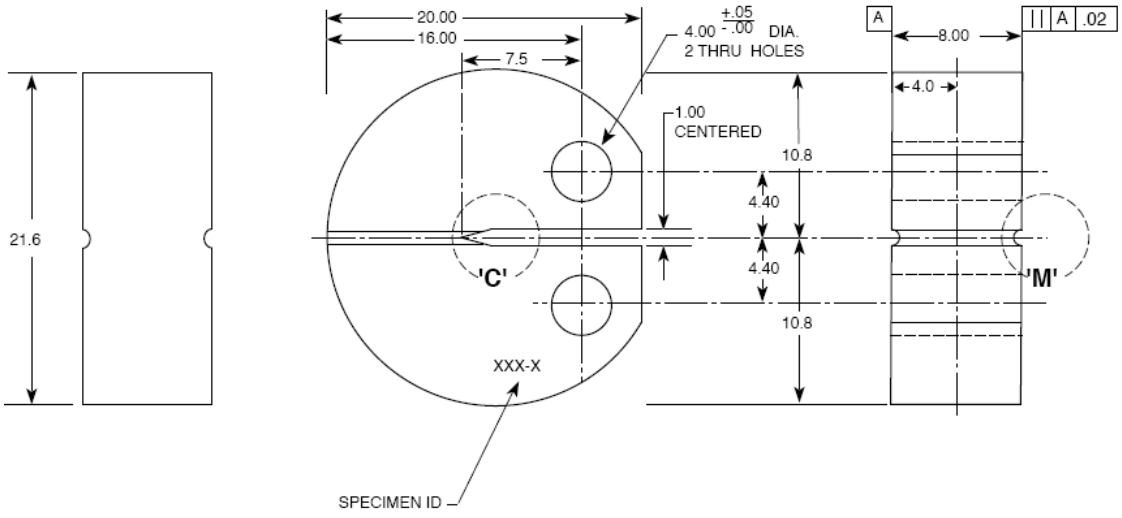

Figure 1. Disk-shaped compact tension specimen used in this study.

2.2 Test Facility and Procedure

The crack growth rate test was performed in a mechanical test facility located in the Irradiated Materials Laboratory (IML) at Argonne National Laboratory. The IML is a radiological laboratory maintained at a negative pressure with respect to the surroundings, and has four shielded hot cells equipped with remote manipulators for handling radioactive materials. The mechanical test facility consists of a loading frame, an Instron 8500+ Dynamic Materials Testing System, and a water recirculation system. During this test, the environment was high-purity deionized water with≈10 ppb DO, i.e. a simulated BWR environment with HWC. The conductivity was 0.06 μS/cm for the feedwater and less than 0.1 μS/cm for the effluent. The flow rate at the autoclave was about 20-30 ml/min. The electrochemical potential (ECP) for SS was between -470 to -560 mV vs. standard hydrogen electrode (SHE).

The CGR test was performed in a one-liter autoclave at 287 and 320°C. The autoclave pressure was maintained at about 1800 psig. The test was conducted under a load-control mode. Crack extension was measured by the direct-current potential drop (DCPD) method.

The test procedure includes three basic stages, fatigue precrack, cyclic CGR test, and constant-load CGR test. The entire test was performed in the low-DO environment described above. The test began with a cyclic load with a low load ratio ($R<0.3$) and a high frequency (>1 Hz) to precrack the sample in the environment. The goal was to generate a sharp fatigue crack and extend the crack front beyond the damaged region immediately next to the machine notch. After the precrack stage, a serial of test periods with slow/fast sawtooth waveforms at a constant K_{max} were followed to establish environmentally-enhanced crack growth and transition the fatigue crack to a stress corrosion crack. In this test stage, the load ratio (R) and rise times were increased incrementally. Once the environmentally-enhanced cracking was successfully established, the third test stage was started under a constant load with or without periodic partial unloading. As the crack propagated, the load was gradually reduced to maintain a constant K at the crack front.

After the CGR test, the specimen was subjected to a cyclic load to mark the final crack length. After the sample was broken, optical and scanning electron microscope (SEM) images of the fracture surface were obtained and the final crack length was measured with a 9/8 averaging technique to compare with the DCPD result. Due to unbroken ligaments or uneven crack front, crack extension is likely to be underestimated by the DCPD method. The crack length obtained by DCPD method for each test period was scaled proportionally with the measurement of the final crack length based on the SEM images. The corrected crack length history plots were then used to determine crack growth rate for each test period.

2.3 Maximum Applied Stress

To ensure the SCC CGR is measured under a plane-strain condition, a standard test practice for evaluating a plane-strain fracture toughness (ASTM E399) was used. This test practice requires the specimen thickness, B, and remaining ligament, (W-a), to be greater than $2.5\ (K/\sigma_y)^2$, where K is the applied stress intensity factor and σ_y is the yield stress of the material. With this criterion on the K and specimen size, the plastic zone ahead of the crack tip is embedded within a

sufficiently large elastic singularity zone. It is believed that very high CGRs are anticipated if the applied stress is above the K limit [20].

For irradiated materials, the value of σ_y to be used in the size criterion is still a subject of debate. Due to strain softening in high-dose specimens, the use of an effective yield strength (σ_{eff}), rather than the irradiated yield stress $\sigma_{y\text{-}Irr}$, has been proposed [16, 21]. For moderate to highly irradiated materials, an effective yield stress of $\sigma_{y\text{-}nonIrr} + \Delta\sigma /2$ or $\sigma_{y\text{-}nonIrr} + \Delta\sigma/3$, where $\Delta\sigma=\sigma_{y\text{-}Irr} - \sigma_{y\text{-}nonIrr}$, has been suggested. To help verify the proposed σ_{eff} for the corresponding K/size criteria, constant loads both below and above the maximum allowable K (based on $\sigma_{y\text{-}nonIrr}+\Delta\sigma/3$) were applied. A sudden change in the K dependence of CGR when the K was increased passing the allowable value would indicate the relevance of the proposed K/size criteria.

3. Crack Growth Rate Test and Results

To minimize loose contamination, the specimen was cleaned thoroughly before testing. After the specimen was installed in the autoclave, the system was pressurized and heated slowly while a small tensile load (less than 5 MPa $m^{1/2}$) was maintained on the sample. After the system was pressurized (≈1800 psig) and the test temperature was reached (≈320°C), the sample was soaked in the low-DO water for about 10 days to stabilize environmental conditions. The test was then started with a cyclic loading at R=0.2 and K_{max}=10 MPa $m^{1/2}$. No crack extension was detected until K_{max} was increased to 18 MPa $m^{1/2}$. After about 150 μm crack extension, K_{max} was reduced to 11 MPa $m^{1/2}$. Then, load levels, load ratios and rise times were gradually increased to induce environmental effects. Environmentally enhanced cracking was not readily established in this sample until K_{max} was increased to 14 MPa $m^{1/2}$ at R=0.5. After about an additional 50-μm crack extension, the test was transitioned to a constant-load test at K=15.7 MPa $m^{1/2}$. Figure 2a shows the end of transition stage from the cyclic CGR to constant-load CGR tests.

The constant-load CGR stage began with a test period with a periodic partial unloading every 2 hours at R=0.6. The partial unloading consisted of a load cycle of 12 s down and 12 s up. The DCPD measurement of the test period with a partial unloading every 2 hours yielded a CGR of $1.8x10^{-11}$ m/s. Following this test period, the test was set to a constant load without periodic unloading at the same stress level. A CGR of $1.4x10^{-11}$ m/s was recorded. After about 400 hours at the load level of 15.7 MPa $m^{1/2}$, the load was increased to 19.4 MPa $m^{1/2}$ and the periodic unloading was re-introduced every 2 hrs at R=0.6. The crack was advanced for about 23 μm during this period of time, and the CGR was about $6.1x10^{-11}$ MPa $m^{1/2}$. After the periodic unloading was removed, the CGR became very slow, most probably due to unbroken ligaments or an uneven crack surface. To verify this observation, the test periods with and without unloading were repeated. The obtained CGR with unloading was nearly identical to that measured previously. No crack extension could be seen in the test period without periodic unloading. In the next test period, CGR was measured with a partial unloading every 4 hours. A slightly lower CGR was obtained with a less frequent unloading.

The stress level was increased further in the next test period to 24.6 MPa $m^{1/2}$. Initially, a periodic partial unloading at R=0.6 every 4 hours was employed, and a crack growth rate close to $1.4x10^{-10}$ m/s was recorded. Once the periodic unloading was removed, the measured CGR

dropped an order of magnitude. After about 6 μm crack extension at a constant load, the periodic unloading was restored with a hold time of 2 hours. The obtained CGR was about a factor of two higher than that measured with 4 hours hold time. To evaluate the effect of load ratio, the periodic unloading was also applied at R=0.7 for every 2 and 4 hours respectively. Compared to R=0.6, the CGRs at R=0.7 were about a factor of two lower for both 2 and 4 hours hold times. After about 19 μm crack extension, the K value was increased to 31 MPa $m^{1/2}$. This stress level is just below the maximum allowable K value (33 MPa $m^{1/2}$) determined by using 1/3 of the value of irradiated and nonirradiated yield strengths. Figure 2b shows the test periods at this stress level. With R=0.6, the obtained CGRs for 2 and 4 hours holding times were approximately $5.6x10^{-10}$ m/s and $2.7x10^{-10}$ m/s respectively. The CGR at a higher load ratio of R=0.7 was slightly lower for 4 hours holding time. Finally, the test was set to a constant K at 31.3 MPa $m^{1/2}$, and an average CGR of $2.1x10^{-11}$ m/s was obtained with 42 μm extension.

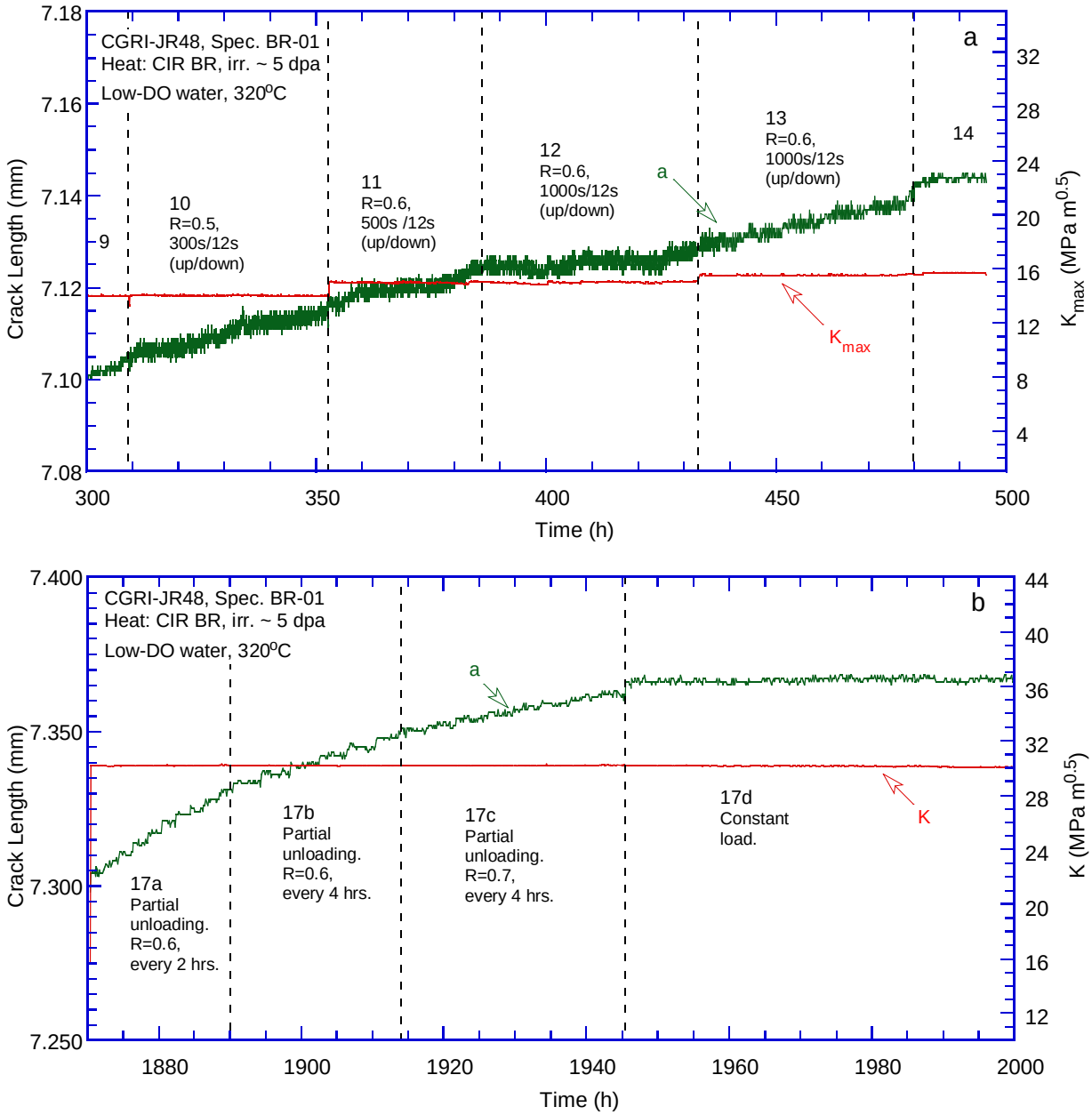

Figure 2. Examples of the crack length history plots obtained in cyclic and constant-load CGR tests: (a) transition from cyclic CGR to constant-load CGR test periods, (b) and (c) constant load test periods below and above the proposed allowable K, respectively.

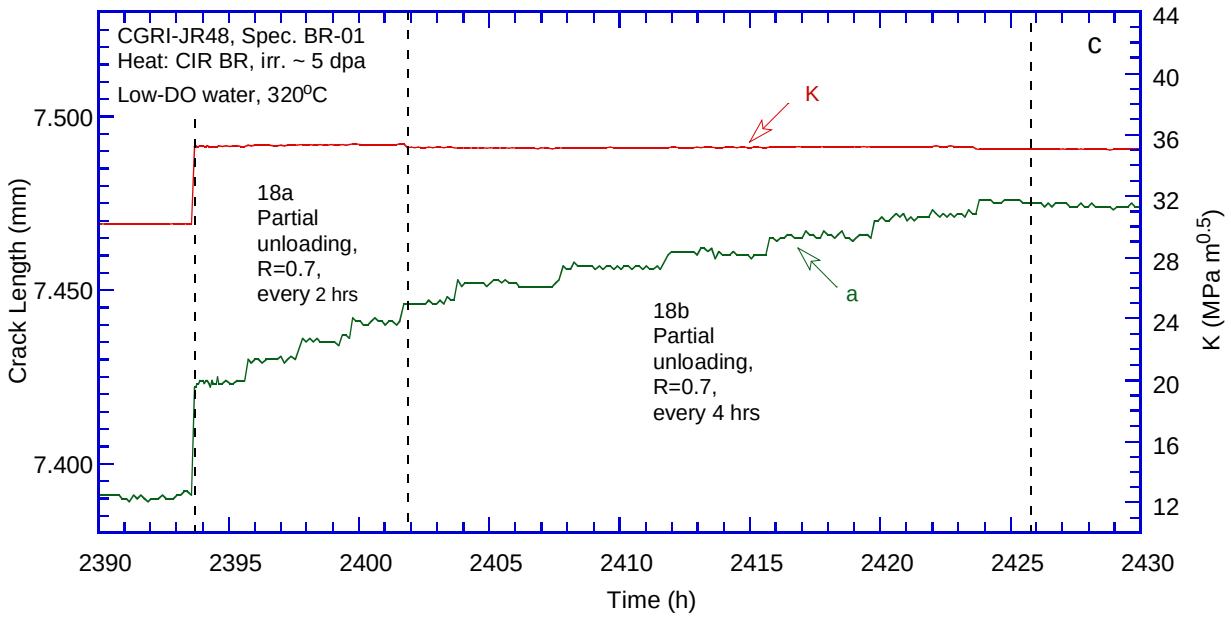

Figure 2. (Continued)

Next, the stress level was increased to 36.9 MPa $m^{1/2}$ (above the maximum allowable value, 33 MPa $m^{1/2}$). Figure 2c shows the test periods at this stress level. Initially, a periodic partial unloading of R=0.7 was applied every 2 hours. The obtained CGR was about $1x10^{-9}$ m/s. After the frequency of periodic unloading was reduced to every 4 hours, the CGR was roughly a factor of two lower. Finally, the test was set to a constant load without unloading, and a CGR of $2.4x10^{-11}$ m/s was registered with approximately 13 μm crack extension. It is also noted that, during the test periods with periodic unloading, a stepped crack growth behavior was observed. While a substantial crack advance occurred right after an unloading cycle, the measured CGR during the hold time (2 or 4 hours) were minimum.

After the CGR test at 320°C, a short test period was performed at 290°C to evaluate the temperature dependence of crack growth behavior in the low-DO environment. The system temperature was reduced and stabilized around 288°C. Crack growth rates were then measured at K=31.6 MPa $m^{1/2}$ (below the proposed K limit) with periodic unloading every 2 and 4 hours respectively. Finally, the test was set to a constant load without periodic unloading. After approximately 200 hours, the CGR test was concluded and a CGR of $6.9x10^{-12}$ m/s was measured for the constant-load test period.

After the CGR test, fatigue cyclic loading was applied to mark the final crack length, and then the sample was pulled apart in tension. The sample failed unexpectedly at a very small strain, suggesting severe irradiation embrittlement of this material. After the sample was broken open, a post-test SEM examination was performed on the fracture surface. The measured crack size was about 39% greater than that estimated by DCPD measurement. And thus, the crack extension determined by the DCPD was scaled proportionally to match the final crack size.

4. Discussion

4.1 Cyclic Crack Growth Rate

The cyclic CGRs obtained from this specimen are shown in Fig. 3. Only the test periods with more than 10 μm crack extension are included in the figure. For the initial fatigue loading, no crack extension was detected until the K_{max} was increased to 18 MPa $m^{1/2}$. This observation is consistent with the result from a previous study performed by Jenssen on the same material irradiated to 25 dpa [15]. The difficulty involved in establishing environmental effect in this CW sample was unexpected, and several attempts by adjusting load ratios and rise times had to be made to introduce environmentally enhanced cracking. It appears that environmentally assisted cracking was difficult to sustain at a low stress level for this sample. However, once the enhanced cracking was established, the cyclic CGR behavior was similar to other irradiated SSs.

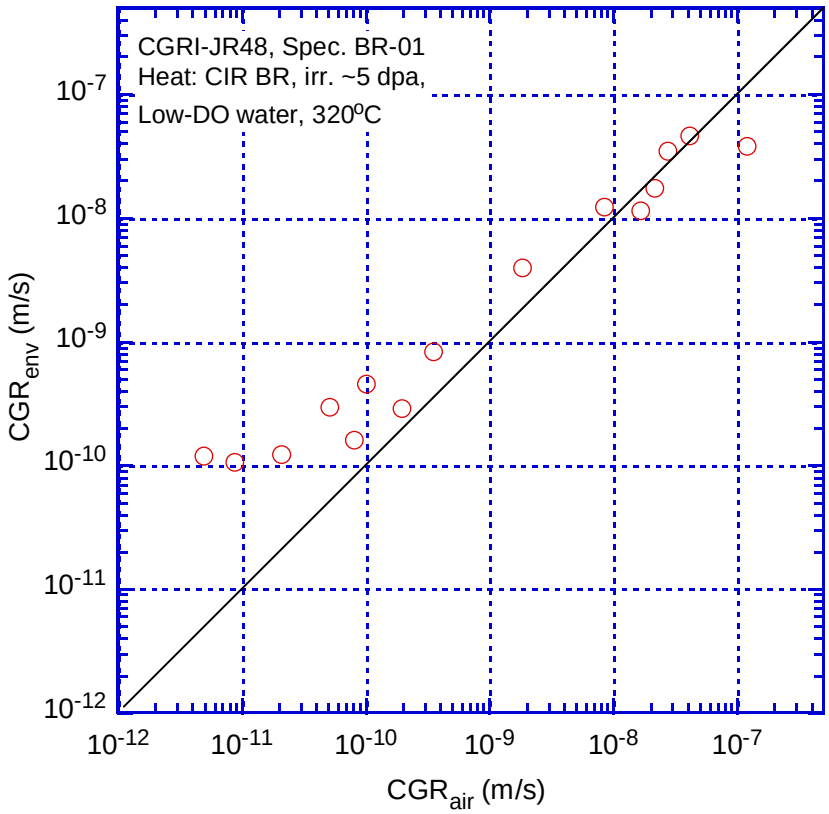

Figure 3. Cyclic CGRs of a 5-dpa Type 316 CW specimen in low-DO environment.

4.2 SCC Growth Rate

Crack growth rates measured during constant-load test periods (with or without periodic unloading) were plotted in Fig. 4. The NUREG-0313 curve was also included as a reference. Despite the very mild periodic unloading (R=0.6-0.7), CGRs with or without unloading are significantly different. This behavior is quite different from the CGR tests in BWR NWC where periodic unloading seems to have an insignificant effect on the CGRs [13,14]. It is possible that unbroken ligaments or uneven cracking surface have influenced the DCPD measurements in

low-DO environment. Crack extension without unloading may have been masked by linkages or contacts of uneven fracture surface. Only with a gentle unloading cycle, can these weak linkages or surface contacts be opened, and thus a higher average crack growth rate revealed.

The stair-step crack growth is a phenomenon not usually seen in NWC tests. In low-DO environments, this effect may be associated with a dynamic strain condition resulting from partial unloading. While the stepped crack growth was clearly observed during the portion of the test in which the applied K was greater than the maximum allowable K, the effect was not limited to the high K region only. A careful analysis of all test periods with periodic unloading shows that the CGRs for a 2 hours hold time are all about a factor of two greater than the CGRs with 4 hours hold time. This suggests that although small, the stepped crack growth under periodic unloading also occurred at lower stress intensity levels.

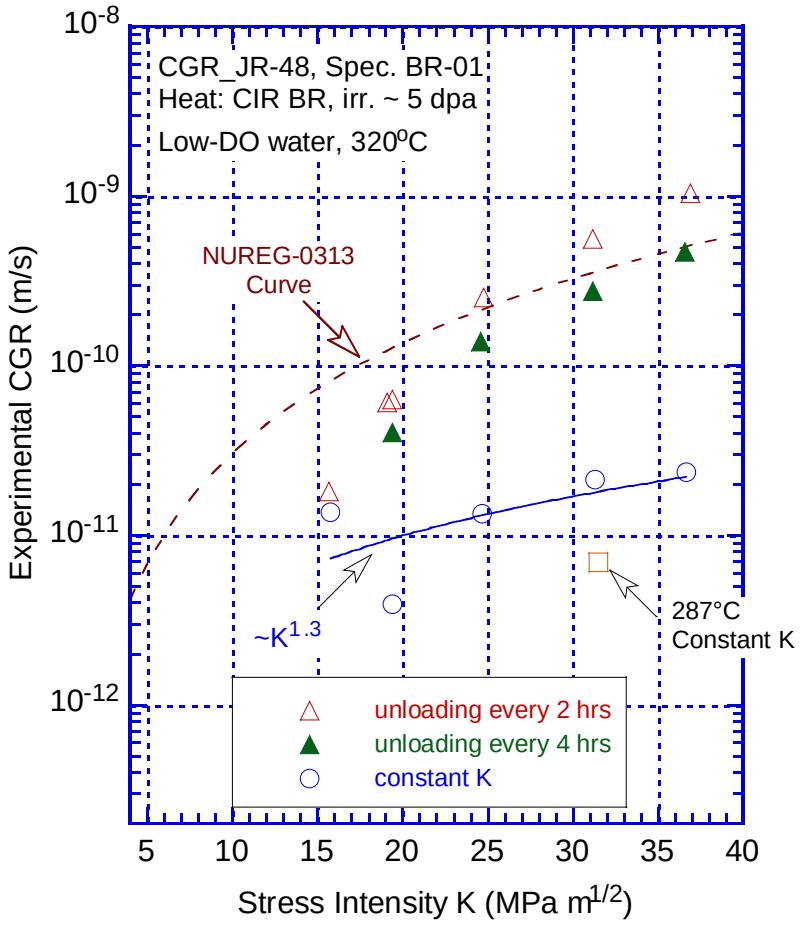

Figure 4. SCC CGRs of a 5-dpa Type 316 CW specimen in low-DO environment (R=0.7 for the unloading at 37 MPa $m^{1/2}$, R=0.6 for all the rest unloading plotted).

A few low-DO CGR tests reported previously on 3-dpa specimens are compared with the current result in Fig. 5 [13,22]. The tests with periodic unloading or varying K seem associated with much higher growth rates in the figure. The K dependence of CGR with periodic unloading or varying K is also much stronger than that of constant K. These different cracking behaviors imply a significant role of dynamic loading condition in SCC. The fact that K dependence is sensitive to hold time also confirms the important role of a dynamic straining in low-DO tests. Andersen has discussed in detail how the dynamic strain might contribute to cracking under SCC or corrosion fatigue conditions [20]. In the current test, when a dynamic loading condition is

absent, beneficial effect of HWC can be observed as shown by the low growth rates under constant K. With periodic unloading the CGR can be elevated considerably in a low-DO environment. Nonetheless, the effective stress of $\sigma_{y\text{-}nonIrr} + \Delta\sigma/3$ seems to be too conservative for the K/size criterion, because the K dependence of CGR is nearly unchanged when the applied K increases beyond the proposed allowable limit.

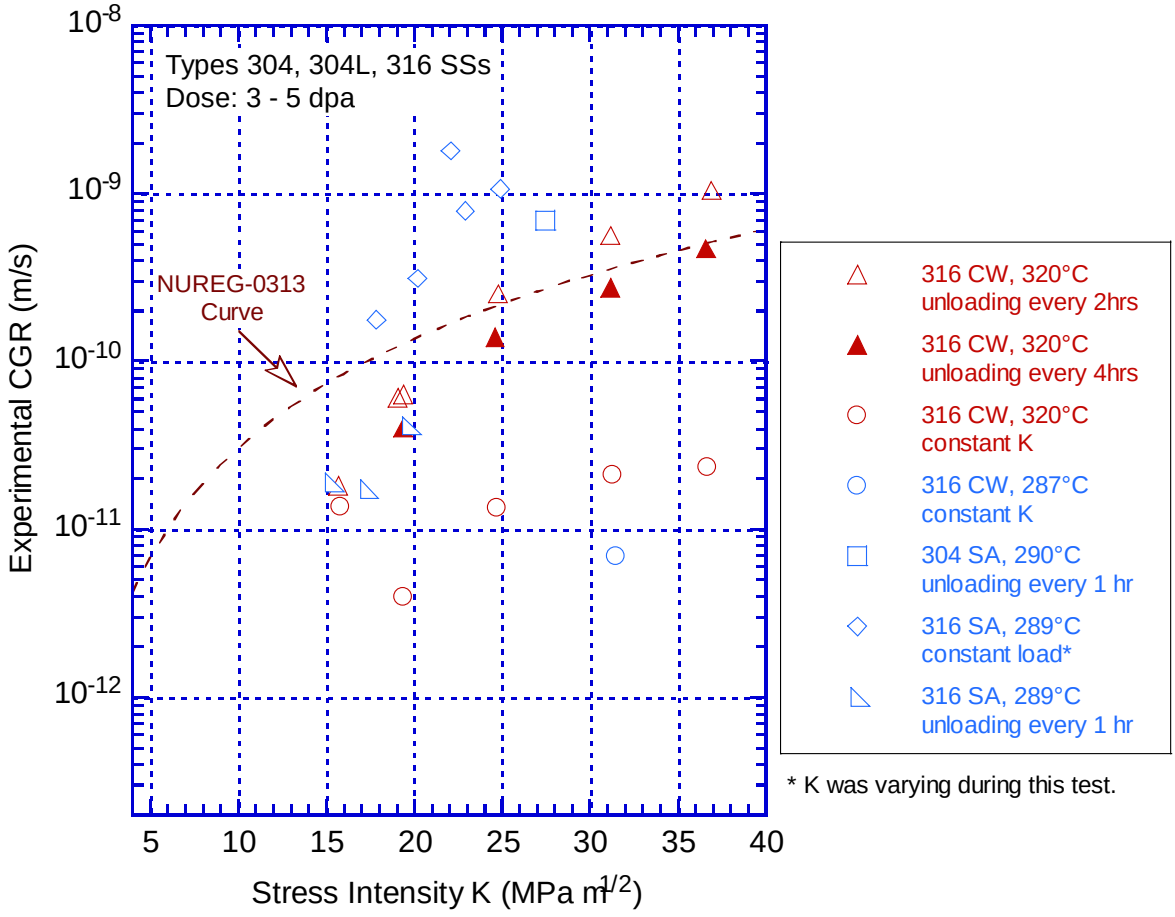

Figure 5. CGR tests in low-DO environments on specimens irradiated to 3-5 dpa [13,22].

4.3 Temperature Dependence

Constant-load CGRs measured at 320°C and 287°C without periodic unloading were plotted in an Arrhenius type plot as shown in Fig. 6. The apparent activation energy of 111 kJ/mol was estimated for this material. This result is lower than that measured by Studsvik (154 kJ/mol) on the same material irradiated to a higher dose (25 dpa) [15], but similar to the value reported for nonirradiated CW 316 SS (~100 kJ/mol) [23].

4.4 Fracture Surface Examination

After several steps of cleaning and decontamination, the tested specimen was transferred to a shielded SEM for examination. Figure 7 shows the entire crack front of the specimen. It appears that the specimen was heavily deformed in the direction of crack propagation. Elongated deformation microstructure along the rolling direction was clearly visible in the area beyond the CGR test region.

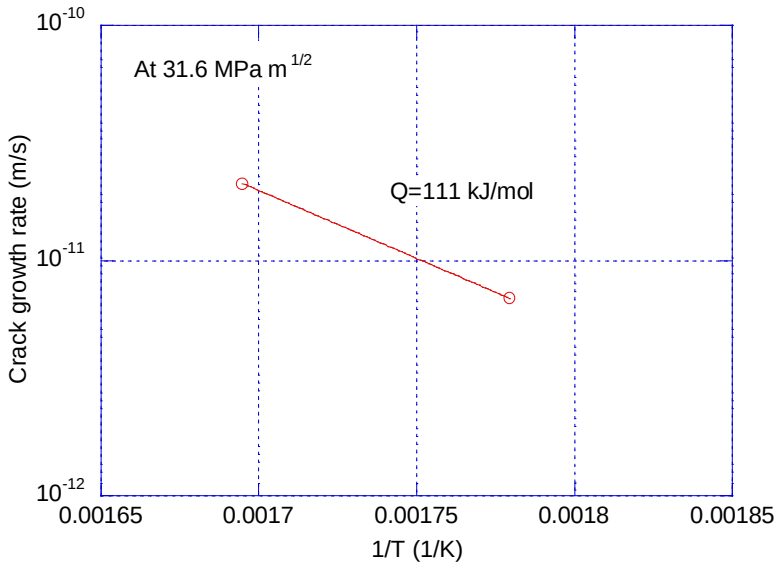

Figure 6. Temperature dependence of CGR behavior in low-DO environment.

Figure 7. Crack front of the Type 316 CW specimen irradiated to 5 dpa, tested in low-DO water.

In the CGR test region, transgranular fracture was dominant in the initial part of crack extension. This can be attributed to aggressive cyclic loading at the beginning of the test. Gradually, intergranular fracture started to develop with a slow reduction of mechanical fatigue component. It appears that IG cracking was developed initially on one side of sample than another, but eventually the entire crack front became predominant IG. Detail images of IG cracking region are shown in Fig. 8. Mixed mode fracture can be seen towards the end of the CGR test where applied stress was approaching or beyond the maximum allowed K (Fig. 9). The deformation band structure was still visible along with IG cracking, suggesting unbroken ligaments were present during crack propagation. Beyond the CGR test region, the elongated deformation microstructure became the dominant morphology.

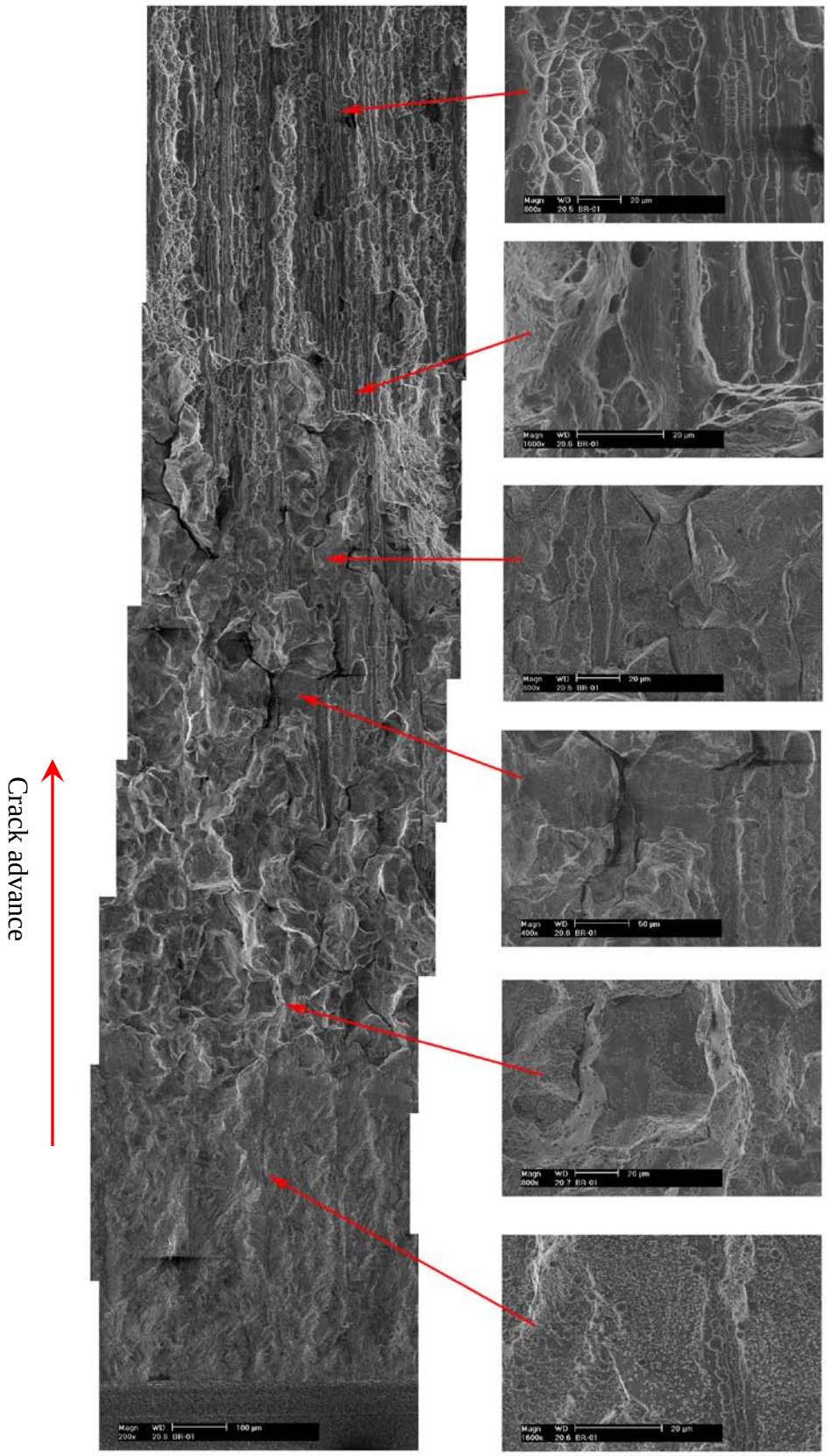

Figure 8. Microstructure of fracture surface of the Type 316 CW specimen irradiated to 5 dpa, tested in low DO water.

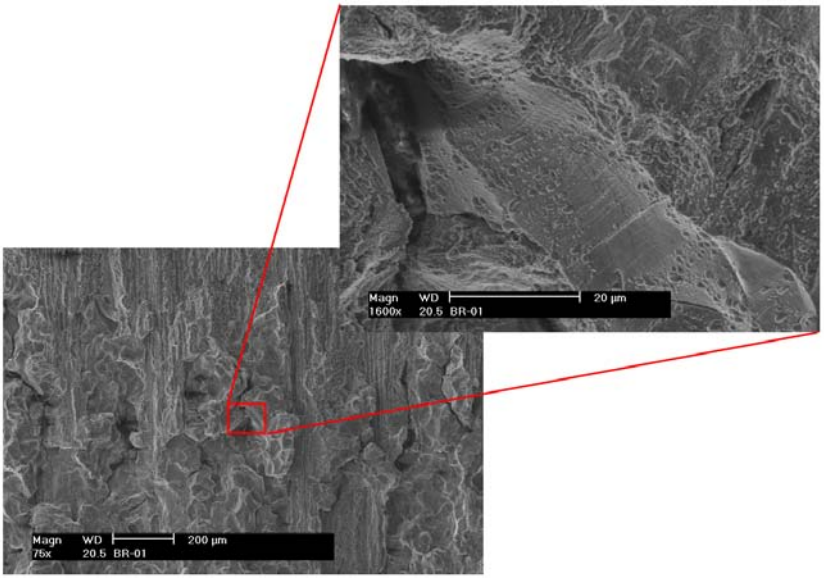

Figure 9. Mixed mode fracture in the Type 316 CW specimen irradiated to 5 dpa, tested in low-DO environment.

5. Conclusions

A crack growth rate test was performed on a DCT Type 316 CW specimen in low-DO environment. The specimen was irradiated to 4.8 dpa in the BOR60 reactor at 320°C. Crack growth rates were obtained at several stress intensity levels with and without periodic unloading. A temperature dependence of CGR was also obtained, and the apparent activation energy was estimated. Fractographic examination showed intergranular and mixed mode fracture in the CGR test region. Despite the heavily deformed microstructure and irradiation damage, cracking susceptibility of this material was moderate in the low-DO environment. Benefit effect of low potential can be observed in this sample without periodic unloading. Dynamic strain resulting from periodic unloading is critical for the SCC behavior in a low-DO environment.

Acknowledgements

The authors would like to thank O. K. Chopra for his invaluable contributions to this program. We'd like to thank Dr. Raj Pathania for providing the sample through the Cooperative IASCC Research (CIR) program. We also want to thank Mr. Anders Jenssen for arranging sample transfer. L. A. Knoblich, E. J. Listwan, W. K. Soppet, D. L. Rink, and R. Clark are acknowledged for their contributions to the experimental effort. This work is sponsored by the Office of Nuclear Regulatory Research, U.S. Nuclear Regulatory Commission, under Job Code N-6519; Program Manager: Appajosula S. Rao.

References

1. Craig F. Cheng, "Intergranular Stress-Assisted Corrosion Cracking of Austenitic Alloys in Water-Cooled Nuclear Reactors", J. Nucl. Mater., **56** (1975)11-33.

2. F. Garzarolli, H. Rubel, and E. Steinberg, “Behavior of Water Reactor Core Materials with Respect to Corrosion Attack,” Proc. Intl. Symp. on Environmental Degradation of Materials in Nuclear Power Systems - Water Reactors, NACE, Houston, TX, pp. 1-24, 1984.

3. F. Garzarolli, D. Alter, and P. Dewes, “Deformability of Austenitic Stainless Steels and Nickel-Base Alloys in the Core of a Boiling and a Pressurized Water Reactor,” Proc. Intl. Symp. on Environmental Degradation of Materials in Nuclear Power Systems - Water Reactors, American Nuclear Society, La Grange Park, IL, p. 131-138, 1986.

4. R. L. Jones, J. D. Gilman, J. L. Nelson, “Controlling stress corrosion cracking in Boiling Water reactors,” J. Nucl. Mater., **143** (1993) 111.

5. A. J. Jacobs, G. P. Wozadlo, K. Nakata, T. Yoshida, and I. Masaoka, “Radiation Effects on the Stress Corrosion and Other Selected Properties of Type-304 and Type-316 Stainless Steels,” Proc. 3rd Intl. Symp. Environmental Degradation of Materials in Nuclear Power Systems--Water Reactors, G. J. Theus and J. R. Weeks, eds., The Metallurgical Society, Warrendale, PA, pp. 673-680, 1988.

6. G. M. Gordon, and K. S. Brown, “Dependence of Creviced BWR Component IGSCC Behavior on Coolant Chemistry”, Proc. 4th Intl. Symp. on Environmental Degradation of Materials in Nuclear Power Systems--Water Reactors, NACE, Houston, TX, pp. 1.4.46-14.62, 1990.

7. F. Garzarolli, D. Alter, P. Dewes, and J. L. Nelson, “Deformability of Austenitic Stainless Steels and Ni-Base Alloys,” Proc. 3rd Intl. Symp. on Environmental Degradation of Materials in Nuclear Power Systems--Water Reactors, G. J Theus and J. R. Weeks, eds., The Metallurgical Society, Warrendale, PA, pp. 657-664, 1988. 8. P. Scott, “A Review of Irradiation Assisted Stress Corrosion Cracking”, J. Nucl. Mater., 211, 101-122, 1994.

9. G. S. Was, and P. L. Andresen, “Stress Corrosion Cracking Behavior of Alloys in Aggressive Nuclear Reactor Core Environments,” Corrosion, **Vol. 63**, No.1, (2007), 19.

10. P. L. Andresen, F. P. Ford, S. M. Murphy, and J. M. Perks, “State of Knowledge of Radiation Effects on Environmental Cracking in Light Water Reactor Core Materials,” Proc. 4th Intl. Symp. on Environmental Degradation of Materials in Nuclear Power Systems--Water Reactors, NACE, Houston, TX, pp. 1.83-1.121, 1990.

11. S. Hettlarachchi “BWR SCC Mitigation Strategies and Their Effectiveness,” Proc. 11th Intl. Symp. on Environmental Degradation of Materials in Nuclear Power Systems, NACE, (2003)

12. M. L. Castano, M. Nacas, D. Gomez-Briceno, T. Onchi, K. Hide, “IASCC response of sensitized 304 Stainless Steels to the Hydrogen Injection in BWR,” Proc. 10th Intl. Symp. on Environmental Degradation of Materials in Nuclear Power Systems--Water Reactors, NACE, (2001)

13. O. K. Chopra, and W.J. Shack, “Crack Growth Rates and Fracture Toughness of Irradiated Austenitic Stainless Steels in BWR Environments,” NUREG/CR-6960, ANL-06/58, 2008.

14. Y. Chen, W. J. Shack, B. Alexandreanu, E. E. Gruber, A. S. Rao, “Cracking Behavior of Irradiated Heat-Affected Zone Specimens of Type 304 and 304L Stainless Steel Welds in High-Purity Water,” Proc. 14th Int. Conf. on Environmental Degradation of Materials in Nuclear Power Systems, Virginia Beach, VA, August 23-27, 2009.

15. A. Jenssen, J. Stjarnsater, R. Pathania, “Crack growth rate testing of fast reactor irradiated Type 304L and 316 SS in BWR and PWR environments,” Proc. 14th Int. Conf. on

Environmental Degradation of Materials in Nuclear Power Systems, Virginia Beach, VA, August 23-27, 2009

16. A. Jenssen, P. Efsing, K. Gott, P. O. Andersson, “Crack Growth Behavior of Irradiated Type 304L Stainless Steel in Simulated BWR Environment,” Proc. 11th Intl. Symp. on Environmental Degradation of Materials in Nuclear Power Systems--Water Reactors, NACE, (2003)

17. O. K. Chopra, B. Alexandreanu, E. E. Gruber, W. J. Shack, “Crack Growth Behavior of Irradiated Austenitic Stainless Steel Weld Heat Affected Zone Material in High-Purity Water at 289°C,” Proc. 12th Int. Symp. on Environmental Degradation of Materials in Nuclear Power Systems--Water Reactors, TMS, p.289 (2005).

18. T. M. Karlsen, P. Bennett, N.W. Hoegberg, “In-Core Crack Growth Rate Studies on Irradiated Austenitic Stainless Steels in BWR and PWR Conditions in the Halden Reactor,” Proc. 12th Intl. Conf. on Environmental Degradation of Materials in Nuclear Power System – Water Reactors, 2005.

19. Electric Power Research Institute, “CIR II Program: Description of the Boris 6 and 7 Experiment in the BOR-60 Fast Breeder Reactor,” (Report No. 1011787, Palo Alto, CA, 2005).

20. P. L. Andresen, “Unusual Cold Work and strain rate effects on SCC,” 14th Int. Conf. on Environmental Degradation of Materials in Nuclear Power Systems, Virginia Beach, VA, August 23-27, 2009.

21. P. L. Andresen, “K/Size Effects on SCC in Irradiated, Cold-Worked and Unirradiated Stainless Steel”, 11th Int. Conf. Environmental Degradation of materials in Nuclear Systems, Stevenon, WA, 2003

22. O. K. Chopra, E. E. Gruber, and W.J. Shack, “Fracture Toughness and Crack Growth Rates of Irradiated Austenitic Stainless Steels,” NUREG/CR-6826, ANL-03/22, 2003.

23. Koji Arioka, Takuyo Yamada, Takumi Terachi, and Tomoki Miyamoto, “Temperature, Potential and Sensitization Effects on Intergranular Crack Growth and Crack-tip appearance of Cold Worked 316,” 13th International Conference on Environmental Degradation of Materials in Nuclear Power Systems, 2007